

General Disclaimer

One or more of the Following Statements may affect this Document

- This document has been reproduced from the best copy furnished by the organizational source. It is being released in the interest of making available as much information as possible.
- This document may contain data, which exceeds the sheet parameters. It was furnished in this condition by the organizational source and is the best copy available.
- This document may contain tone-on-tone or color graphs, charts and/or pictures, which have been reproduced in black and white.
- This document is paginated as submitted by the original source.
- Portions of this document are not fully legible due to the historical nature of some of the material. However, it is the best reproduction available from the original submission.

(NASA-CR-145266) STRESS-INTENSITY FACTORS
FOR A THICK-WALLED CYLINDER CONTAINING AN
ANNULAR IMBEDDED OR EXTERNAL OR INTERNAL
SURFACE CRACK (Lehigh Univ.) 25 p HC A02/MF
A01

N78-10509

Unclas
51859

CSCL 20K G3/39

STRESS-INTENSITY FACTORS FOR A THICK-WALLED
CYLINDER CONTAINING AN ANNULAR IMBEDDED OR
EXTERNAL OR INTERNAL SURFACE CRACK

by

RAGIP ERDOL

and

F. ERDOGAN.

August 1976

Lehigh University

The National Aeronautics and Space
Administration Grant No. NGR39-007-011



STRESS-INTENSITY FACTORS FOR A THICK-WALLED
CYLINDER CONTAINING AN ANNULAR IMBEDDED OR
EXTERNAL OR INTERNAL SURFACE CRACK*

by

Ragip Erdol ** and F. Erdogan
Lehigh University, Bethlehem, PA

Abstract. The paper considers the elastostatic axisymmetric problem for a long thick-walled cylinder containing a ring-shaped internal or edge crack. Using the standard transform technique the problem is formulated in terms of an integral equation which has a simple Cauchy kernel for the internal crack and a generalized Cauchy kernel for the edge crack as the dominant part. As examples the uniform axial load and the steady-state thermal stress problems have been solved and the related stress intensity factors have been calculated. Among other findings the results show that in the cylinder under uniform axial stress containing an internal crack the stress intensity factor at the inner tip is always greater than that at the outer tip for equal net ligament thicknesses and in the cylinder with an edge crack which is under a state of thermal stress the stress intensity factor is a decreasing function of the crack depth, tending to zero as the crack depth approaches the wall thickness.

1. INTRODUCTION

In studying the fracture problem in pressure vessels, pipes, and other cylindrical containers, if the wall thickness relative to the mean radius is sufficiently small, the related crack problem may be solved by assuming the structure to be a shallow shell. In this case the problems which lend themselves to analytical treatment are those involving relatively short circumferential and axial through cracks in (infinitely) long cylindrical shells (for review and references see, for example, [1]). The problems of a through crack in a thick-walled cylinder and a part-through crack of finite size in a thick or thin-

* This work was partly supported by NSF under the Grant ENG-73 045053 A01 and by NASA-Langley under the Grant NGR39-997-011.

** Permanent address: Black Sea Technical University, Trabzon, Turkey.

walled cylinder at the present time do not appear to be tractable. Nevertheless, these are the practical problems. Therefore, it would be of some interest if one can provide bounds for or give some idea about the magnitude and the trends of certain relevant quantities such as the stress intensity factors by solving the problem under certain idealized conditions regarding the crack geometry and the loading. One of the simplest of such idealized problems is considered in this paper. If (a) the flaw in the cylinder is a part-through circumferential crack lying in a plane perpendicular to the axis, (b) the radial dimension of the flaw is relatively constant and its circumferential dimension is large compared to the wall thickness, and (c) the external loads are axisymmetric, then the axisymmetric ring-shaped crack shown in Figure 1 may approximate the problem around the center portion of the flaw. From the viewpoint of fracture propagation, since this mid-portion of the flaw is the most critical location, the approximate solution thus found would be very useful. The ring-shaped crack may be an internal crack ($a < c < d < b$), an edge crack on the inner surface ($a = c < d < b$), or an edge crack on the outer surface ($a < c < d = b$) (see Figure 1). Once the governing integral equation is obtained, the problem can be solved for any axisymmetric quasistatic external load. In this paper the results will be given for uniform axial loading and for steady-state temperature distribution.

The corresponding problem for the solid cylinder with a penny-shaped crack (i.e., $a = 0 = c$) was treated in [2-4], and for the strip with internal or edge cracks in [5].

2. DERIVATION OF THE INTEGRAL EQUATION

Consider the problem for a long thick-walled cylinder which contains a concentric ring-shaped crack in $z=0$ plane, z being the axis of the cylinder (see Figure 1). Let the cylinder be subjected to (quasi-static) axisymmetric external loads which may be mechanical, thermal, or residual in nature and are independent of z . In the absence of the crack let the stress components at $z=0$ be

$$\sigma_{zz}^1(r,0) = f(r) \quad , \quad \sigma_{rz}^1(r,0) = 0 \quad , \quad a < r < b \quad , \quad (1)$$

where $f(r)$ is a known function. If the cylinder is sufficiently long the solution of the cylinder containing the crack may be obtained by superposition, namely, by adding to the (homogeneous) solution of the cylinder without the crack and under given external loads a perturbation solution obtained for the cracked cylinder in which self-equilibrating crack surface tractions are the only external loads. These tractions are equal and opposite to the stress given by (1). From the viewpoint of fracture, the relevant problem is the latter. Therefore, only the perturbation problem will be considered in this paper.

In terms of the Love function $\chi(r,z)$ the axisymmetric problem may be formulated as follows [6]:

$$\nabla^4 \chi = 0 \quad , \quad (2)$$

$$u(r,z) = -\frac{1}{2\mu} \frac{\partial^2 \chi}{\partial r \partial z} \quad , \quad w(r,z) = \frac{1}{2\mu} \left[2(1-\nu) \nabla^2 \chi - \frac{\partial^2 \chi}{\partial z^2} \right] \quad , \quad (3)$$

$$\sigma_{rr} = \frac{\partial}{\partial z} \left[\nu \nabla^2 \chi - \frac{\partial^2 \chi}{\partial r^2} \right] , \quad \sigma_{zz} = \frac{\partial}{\partial z} \left[(2-\nu) \nabla^2 \chi - \frac{\partial^2 \chi}{\partial z^2} \right] , \quad (4)$$

$$\sigma_{rz} = \frac{\partial}{\partial r} \left[(1-\nu) \nabla^2 \chi - \frac{\partial^2 \chi}{\partial z^2} \right] , \quad \sigma_{\theta\theta} = \frac{\partial}{\partial z} \left(\nu \nabla^2 \chi - \frac{1}{r} \frac{\partial \chi}{\partial r} \right) ,$$

where u and w are r and z -components of the displacement vector, μ is the shear modulus, and ν is the Poisson's ratio. For an axisymmetric elastic cylinder in which $z=0$ is a plane of symmetry and the stress state vanishes at $z=\pm\infty$ the biharmonic function χ may be expressed as

$$\begin{aligned} \chi(r,z) = & \frac{2}{\pi} \int_0^\infty [f_1(s) I_0(rs) + f_2(s) rs I_1(rs) \\ & + f_3(s) K_0(rs) + f_4(s) rs K_1(rs)] \sin zs \, ds \\ & + \int_0^\infty f_5(p) p (2\nu+zp) e^{-zp} J_0(rp) dp , \end{aligned} \quad (5)$$

where the functions f_1, \dots, f_5 are unknown. From (3), (4), and (5) the displacements and the relevant stress components are found to be

$$\begin{aligned} u(r,z) = & -\frac{1}{2\mu} \left\{ \frac{2}{\pi} \int_0^\infty [f_1(s) I_1(rs) + f_2(s) rs I_0(rs) \right. \\ & - f_3(s) K_1(rs) - f_4(s) rs K_0(rs)] s^2 \cos zs \, ds \\ & \left. - \int_0^\infty f_5(p) p^3 (1-2\nu-zp) e^{-zp} J_1(rp) dp \right\} , \end{aligned} \quad (6)$$

$$\begin{aligned} w(r,z) = & \frac{1}{2\mu} \left\{ \frac{2}{\pi} \int_0^\infty [f_1(s) I_0(rs) + f_2(s) [4(1-\nu) I_0(rs) \right. \\ & \left. + rs I_1(rs)] + f_3(s) K_0(rs) + f_4(s) [rs K_1(rs) \right. \end{aligned}$$

$$\begin{aligned}
& - 4(1-\nu)K_0(rs)]s^2 \sin zs \, ds \\
& - \int_0^\infty f_5(p)p^3[2(1-\nu)+zp]e^{-zp}J_0(rp)dp \} \tag{7}
\end{aligned}$$

$$\begin{aligned}
\sigma_{rr}(r,z) = & \frac{2}{\pi} \int_0^\infty \{s^2 f_1(s)[-sI_0(rs) + I_1(rs)/r] \\
& + s^3 f_2(s)[(2\nu-1)I_0(rs) - rsI_1(rs)] \\
& - s^2 f_3(s)[sK_0(rs) + K_1(rs)/r] + s^3 f_4(s)[(1-2\nu)K_0(rs) \\
& - rsK_1(rs)]\} \cos zs \, ds + \int_0^\infty p^3 f_5(p)[p(1-zp)J_0(rp) \\
& - (1-2\nu-zp)J_1(rp)/r]e^{-zp} dp \, , \tag{8}
\end{aligned}$$

$$\begin{aligned}
\sigma_{zz}(r,z) = & \frac{2}{\pi} \int_0^\infty \{f_1(s)I_0(rs) + f_2(s)[2(2-\nu)I_0(rs) + rsI_1(rs)] \\
& + f_3(s)K_0(rs) + f_4(s)[rsK_1(rs) - 2(2-\nu)K_0(rs)]\} \cos zs \, ds \\
& + \int_0^\infty p^4 f_5(p)(1+zp)e^{-zp}J_0(rp)dp \, , \tag{9}
\end{aligned}$$

$$\begin{aligned}
\sigma_{rz}(r,z) = & \frac{2}{\pi} \int_0^\infty \{f_1(s)I_1(rs) + f_2(s)[rsI_0(rs) + 2(1-\nu)I_1(rs)] \\
& - f_3(s)K_1(rs) + f_4(s)[-rsK_0(rs) + 2(1-\nu)K_1(rs)]\} s^3 \sin zs \, ds \\
& + \int_0^\infty p^5 f_5(p)ze^{-zp}J_1(rp)dp \, . \tag{10}
\end{aligned}$$

In the crack problem shown in Figure 1 the following are the boundary conditions:

$$\sigma_{rr}(a,z) = 0 \quad , \quad \sigma_{rz}(a,z) = 0 \quad , \quad 0 \leq z < \infty \quad , \quad (11)$$

$$\sigma_{rr}(b,z) = 0 \quad , \quad \sigma_{rz}(b,z) = 0 \quad , \quad 0 \leq z < \infty \quad , \quad (12)$$

$$\sigma_{rz}(r,0) = 0 \quad , \quad a \leq r \leq b \quad , \quad (13)$$

$$\left. \begin{aligned} \sigma_{zz}(r,0) &= -f(r) \quad , \quad c < r < d \quad , \\ w(r,0) &= 0 \quad , \quad a \leq r < c \quad , \quad d < r \leq b \end{aligned} \right\} \quad (14)$$

From (10) it may be observed that the condition (13) is satisfied by the solution (5). The four homogeneous conditions (11) and (12) may be used to eliminate four of the unknowns f_1, \dots, f_5 and the mixed boundary conditions (14) may be used to obtain a system of dual integral equations for the fifth unknown function. Thus, using (8) and (10) the boundary conditions (11) may be expressed as

$$\begin{aligned} & f_1(s) [-sI_0(as) + I_1(as)/a] + sf_2(s) [(2\nu-1)I_0(as) - asI_1(as)] \\ & - f_3(s) [sK_0(as) + K_1(as)/a] + sf_4(s) [(1-2\nu)K_0(as) - asK_1(as)] \\ & = \frac{1}{s^2} \int_0^\infty \frac{p^4 f_5(p)}{p^2 + s^2} \{pJ_0(ap) - (1-2\nu)J_1(ap)/a \\ & + [pJ_0(ap) - J_1(ap)/a] \frac{s^2 - p^2}{s^2 + p^2}\} dp \quad , \end{aligned} \quad (15)$$

$$\begin{aligned}
& f_1(s)I_1(as) + f_2(s)[asI_0(as) + 2(1-\nu)I_1(as)] \\
& - f_3(s)K_1(as) + f_4(s)[2(1-\nu)K_1(as) - asK_0(as)] \\
& = -\frac{1}{s^3} \int_0^\infty \frac{2sp^6 f_5(p)}{(p^2+s^2)^2} J_1(ap) dp \quad . \quad (16)
\end{aligned}$$

Conditions (12) give two more equations which may be obtained from (15) and (16) by replacing a by b . Now, rather than substituting f_1, \dots, f_4 given by these four equations into (14) and obtaining a system of dual integral equations for $f_5(p)$, the problem may be reduced to a singular integral equation in terms of a new unknown function defined by

$$\frac{\partial}{\partial r} w(r,0) = g(r) \quad . \quad (17)$$

From (7), (17), and the second equation of (14) it follows that

$$p^3 f_5(p) = \frac{\mu}{1-\nu} \int_c^d tg(t)J_1(pt)dt \quad . \quad (18)$$

If we now solve (15), (16) and two similar equations for $r=b$ for f_1, \dots, f_4 in terms of $g(t)$ by using (18) and substitute the results into the first equation of (14), by using again (18) and the expression for σ_{zz} as given by (9), after somewhat lengthy but straightforward manipulations, we obtain

$$\int_c^d \left[\frac{1}{t-r} + k(r,t) \right] g(t) dt = -\frac{1-\nu}{\mu} \pi f(r) \quad , \quad c < r < d \quad , \quad (19)$$

where the kernel $k(r,t)$ is given by

$$k(r,t) = k_1(r,t) + 2tk_2(r,t) , \quad (20)$$

$$k_1(r,t) = \frac{m(r,t)-1}{t-r} + \frac{m(r,t)}{t+r} , \quad (21)$$

$$m(r,t) = \begin{cases} E(r/t) , & r < t , \\ \frac{r}{t} E(t/r) + \frac{t^2-r^2}{tr} K(t/r) , & r > t \end{cases} \quad (22)$$

$$k_2(r,t) = \int_0^\infty \frac{ds}{\Delta(s)} \left\{ \left(\sum_1^4 A_i h_i \right) I_0(rs) + \left(\sum_1^4 B_i h_i \right) [2(2-\nu)I_0(rs) \right. \right. \\ \left. \left. + rsI_1(rs)] + \left(\sum_1^4 C_i h_i \right) K_0(rs) + \left(\sum_1^4 D_i h_i \right) [rsK_1(rs) \right. \right. \\ \left. \left. - 2(2-\nu)K_0(rs)] \right\} . \quad (23)$$

Here, K and E are the complete elliptic integrals of first and second kind, respectively and the functions $\Delta(s)$, $A_i(s)$, $B_i(s)$, $C_i(s)$, $D_i(s)$, and $h_i(t,s)$, $(i,1,\dots,4)$ are defined in the Appendix. The expressions of the infinite integrals used in this part of the analysis are given in [7]. From the second equation of (14) and the definition (17) it is clear that the integral equation must be solved under the following single-valuedness condition:

$$\int_c^d g(r)dr = 0 . \quad (24)$$

3. INTERNAL CRACK

A close examination of the kernel $k(r,t)$ defined by (20) to (23) would show that the first part $k_1(r,t)$ has a simple logarithmic singularity (in the form of $\log|t-r|$), whereas the second part $k_2(r,t)$ is bounded in the closed interval $c \leq (r,t) \leq d$ provided $a < c < d < b$, that is if the crack is a fully imbedded internal crack. In this case the Cauchy kernel $1/(t-r)$ is the dominant kernel, the index of the integral equation is +1, the solution is of the form [8]

$$g(r) = G(r) [(r-c)(d-r)]^{-1/2} \quad (25)$$

and, hence a standard numerical technique such as that described in [9] may be used to determine the unknown function $G(r)$ which is bounded in the closed interval $c \leq (r,t) \leq d$. Thus, defining the following normalized quantities

$$r = \frac{d-c}{2} \rho + \frac{d+c}{2} \quad , \quad t = \frac{d-c}{2} \tau + \frac{d+c}{2} \quad ,$$

$$g(r) = \phi(\rho) = F(\rho) (1-\rho^2)^{-1/2} \quad , \quad f(r) = P(\rho) \quad , \quad K(\rho, \tau) = \frac{d-c}{2\pi} k(r, t) \quad (26)$$

equations (19) and (24) may be expressed as

$$\sum_{i=1}^n \frac{1}{n} F(\tau_i) \left[\frac{1}{\tau_i - \rho_j} + \pi K(\rho_j, \tau_i) \right] = - \frac{1-\nu}{\mu} P(\rho_j) \quad ,$$

$$j=1, \dots, n-1 \quad (27)$$

$$\sum_{i=1}^n \frac{\pi}{n} F(\rho_i) = 0 \quad , \quad (28)$$

$$\left. \begin{aligned} \tau_i &= \cos \left(\pi \frac{2i-1}{2n} \right) \quad , \quad i = 1, \dots, n \\ \rho_j &= \cos \frac{\pi j}{n} \quad , \quad j = 1, \dots, n-1 \end{aligned} \right\} \quad (29)$$

After solving the integral equation the stress intensity factors which are defined by

$$\left. \begin{aligned} k(c) &= \lim_{r \rightarrow c} \sqrt{2(c-r)} \sigma_{zz}(r, 0) \quad , \\ k(d) &= \lim_{r \rightarrow d} \sqrt{2(r-d)} \sigma_{zz}(r, 0) \end{aligned} \right\} \quad (30)$$

may be obtained as follows:

$$\left. \begin{aligned} k(c) &= \lim_{r \rightarrow c} \frac{\mu}{1-\nu} \sqrt{2(r-c)} g(r) = \frac{\mu}{1-\nu} \sqrt{(d-c)/2} F(-1) \quad , \\ k(d) &= -\lim_{r \rightarrow d} \frac{\mu}{1-\nu} \sqrt{2(d-r)} g(r) = -\frac{\mu}{1-\nu} \sqrt{(d-c)/2} F(1) \quad . \end{aligned} \right\} \quad (31)$$

where $F(-1)$ and $F(+1)$ are obtained from $F(\tau_i)$, $i=1, \dots, n$, by using the interpolation formulas given in [10].

4. EDGE CRACKS

In the case of edge cracks (i.e., for $a=c<d<b$ or $a<c<d=b$, Figure 1) the integral equation (19) is still valid. However, in this special case the kernel $k(r,t)$ in (19) is no longer bounded in the corresponding

closed interval and, of course, the single-valuedness condition (24) is no longer valid. Therefore, the solution of the problem requires some care. The asymptotic analysis of the integrand in (23) for large values of s indicate that the kernel $k_2(r,t)$ may be expressed as the sum of two parts as follows:

$$k_2(r,t) = k_{2f}(r,t) + k_{2s}(r,t) \quad (32)$$

where k_{2f} is bounded in the corresponding closed interval and k_{2s} becomes unbounded as r and t approach the end point $c=a$ or $d=b$. After some manipulations the asymptotic expressions for the integrand and the singular part of the kernel k_2 are found to be

$$\begin{aligned} k_{2s}(r,t) &= \int_0^{\infty} \frac{ds}{2\sqrt{rt}} [2s^2(r-a)(t-a) - 3s(t-a) \\ &\quad - s(r-a) + 2] e^{-s(r+t-2a)} \\ &= \frac{1}{2\sqrt{rt}} \left[-\frac{1}{r+t-2a} + \frac{6(r-a)}{(r+t-2a)^2} - \frac{4(r-a)^2}{(r+t-2a)^3} \right] \end{aligned} \quad (33)$$

in the neighborhood of the end point a (i.e., for $r-a \ll d-a$ and $t-a \ll d-a$), and

$$\begin{aligned} k_{2s}(r,t) &= -\int_0^{\infty} \frac{1}{2\sqrt{rt}} [2s^2(b-r)(b-t) - 3s(b-t) - s(b-r) \\ &\quad + 2] e^{-s(2b-r-t)} ds \\ &= \frac{1}{2\sqrt{rt}} \left[\frac{1}{2b-r-t} - \frac{6(b-r)}{(2b-r-t)^2} + \frac{4(b-r)^2}{(2b-r-t)^3} \right] \end{aligned} \quad (34)$$

in the neighborhood of the end point b (i.e., for $b-r \ll b-c$ and $b-t \ll b-c$). It should be noted that the singular kernels (33) and (34) are essentially the same as the expressions found for the corresponding plane strain problem considered in [5]. Thus, repeating the analysis of [5], it may be shown that the solution of the integral equation (19), which now has a generalized Cauchy kernel, has no power or logarithmic singularity at the end point which is on the surface and the solution is of the following form

$$\left. \begin{aligned} g(r) &= G_1(r) (d-r)^{-\frac{1}{2}} , \quad a=c < r < d < b , \\ g(r) &= G_2(r) (r-c)^{-\frac{1}{2}} , \quad a < c < r < d=b , \end{aligned} \right\} \quad (35)$$

where G_1 and G_2 are bounded in their respective closed intervals. In this case the stress intensity factors are given by

$$\begin{aligned} k(d) &= -\lim_{r \rightarrow d} \frac{\mu}{1-\nu} \sqrt{2(d-r)} g(r) = -\frac{\sqrt{2\mu}}{1-\nu} G_1(d) , \quad a=c , \\ k(c) &= \lim_{r \rightarrow c} \frac{\mu}{1-\nu} \sqrt{2(c-r)} g(r) = \frac{\sqrt{2\mu}}{1-\nu} G_2(c) , \quad d=b . \end{aligned} \quad (36)$$

The integral equations for the edge cracks may be solved by following the procedure outlined in [5].

5. RESULTS AND DISCUSSION

As an example, the integral equation (19) is solved under two types of input functions, namely, a uniform stress in z direction and a steady

state thermal stress distribution. In the former case

$$\sigma_{zz}^1(r,0) = f(r) = \sigma_0, \quad a \leq r \leq b \quad (37)$$

and in the latter (see, for example, [11])

$$\sigma_{zz}^1(r,0) = f(r) = \sigma_t [1 - 2 \log(b/r) - \frac{2a^2}{b^2 - a^2} \log(b/a)] / \log(b/a) \quad (38)$$

where

$$\sigma_t = \alpha E (T_o - T_i) / 2(1 - \nu), \quad (39)$$

α , E , T_o , and T_i being the coefficient of thermal expansion, Young's modulus, outer wall temperature, and inner wall temperature, respectively. The calculated results are shown in Tables 1-4. Figures 2 and 3 show some sample results which are taken from Tables 3 and 4.

Table 1 shows the normalized stress intensity factor

$$k' = k / (\sigma_0 \sqrt{(d-c)/2}) \quad (40)$$

for a thick-walled cylinder which contains a ring-shaped internal crack along $c < r < d$ and is under uniform axial tension $\sigma_{zz} = \sigma_0$ (Figure 1). It may be seen that as the crack size becomes very small in comparison with other dimensions k' approaches 1 which is the value for a uniformly loaded infinite plane containing a line crack. This was verified by substituting $(d-c)/b = 10^{-5}$ in the program. It may also be observed that if the thicknesses of the net ligaments, $c-a$ and $b-d$ are equal then the stress intensity factor $k(c)$ at the inner tip is always greater than

$k(d)$ at the outer tip, whereas in the corresponding plane problem for a strip they are, of course, equal. The practical consequence of this is that generally one would expect the internal flaws in thick-walled cylinders to propagate inward. Another observation which may be worth mentioning is that, for a fixed c/b , as d/b increases (starting with $d=c$), initially there is a slight reduction in $k'(d)$, then it increases and becomes unbounded as $d \rightarrow b$. However, as seen from (40), the stress intensity factor $k(d)$ itself is proportional to $(d-c)^{1/2}$ and, despite the slight decrease in $k'(d)$, is always an increasing function of the crack size. If $b = \infty$ with a and c finite one would expect that as d increases $k(d)$ would approach $\frac{2}{\pi} \sigma_0 \sqrt{d}$ which is the stress intensity factor for a penny-shaped crack in a uniformly loaded infinite medium. This means that in this case $2/\pi$ is the asymptotic value of $k'(d)$ and $1 > k'(d) > 2/\pi$. For $d-c \ll b$ the reduction in $k'(d)$ is therefore not surprising.

Table 2 shows the normalized stress intensity factors in a thick-walled cylinder with an internal crack which is under a state of steady-state thermal stress given by (38) and (39). Here it is assumed that $T_0 > T_1$, i.e., the cylinder is heated from outside. For again a fixed c , it is seen that as d increases $k'(d)$ decreases and eventually becomes zero as d advances into the compressive stress region. Also as $d \rightarrow c$, $k(d)$ and $k(c)$ approach the local plane strain value i.e., $k(d) \rightarrow f(c) \sqrt{(d-c)/2}$, $k(c) \rightarrow f(c) \sqrt{(d-c)/2}$ where $f(c)$ is the magnitude of the thermal stress σ_{zz} at $r=c$ (see equations 38 and 39). This was again verified by selecting $(d-c)/b = 10^{-5}$.

Table 1. Stress intensity factors in a thick-walled cylinder with an internal crack under uniform axial stress $\sigma_{zz}=\sigma_0$, $k'(d)=k(d)/(\sigma_0 \times \sqrt{(d-c)/2})$, $k'(c) = k(c)/(\sigma_0 \sqrt{(d-c)/2})$.

d/b	a/b=0.3, c/b=0.4		a/b=0.3, c/b=0.5		a/b=0.2, c/b=0.4	
	k'(d)	k'(c)	k'(d)	k'(c)	k'(d)	k'(c)
0.4	→1.0	→1.0			→1.0	→1.0
0.5	0.9973	1.0591	→1.0	→1.0	0.9864	1.0405
0.6	1.0167	1.1493	0.9931	1.0377	0.9963	1.1017
0.7	1.0626	1.2690	1.0150	1.1035	1.0345	1.1900
0.8	1.1645	1.4416	1.0833	1.2098	1.1262	1.3252
0.9	1.4361	1.7374	1.2870	1.4022	1.3726	1.5644
1.0	→∞		→∞		→∞	

Table 2. Stress intensity factors in a thick-walled cylinder with an internal crack under steady state thermal stresses. $k'_t(d)/(\sigma_t \sqrt{(d-c)/2})$, $k'_t(c)/(\sigma_t \sqrt{(d-c)/2})$, $\sigma_t=\alpha E(T_0-T_i)/2(1-\nu)$, a/b=0.3, c/b=0.4.

d/b	0.4	0.401	0.5	0.6	0.7	0.8
$k'_t(d)$	→0.8893	0.8859	0.6044	0.3762	0.1827	0.0093
$k'_t(c)$	→0.8893	0.8885	0.8328	0.7836	0.7279	0.6591

Table 3 shows the normalized stress intensity factors for an edge crack on the inside wall of the cylinder (i.e., a=c, d<b). Here k'(d) refers to the uniform axial loading, $k'_t(d)$ refers to the case of thermal stress. k'(d) is also shown in Figure 2 in order to compare it with plane strain and penny-shaped crack results. It is seen that as $d \rightarrow a$ $k(d) \rightarrow 1.1215 \sigma_0 \sqrt{d-a}$ for uniform axial tension $\sigma_{zz}=\sigma_0$ and $k(d) \rightarrow 1.1215 f(a) \sqrt{d-a}$ for thermal stress f(r) given by (38).^{*} Note that for a half

^{*}The limiting values of the stress intensity factors for the edge cracks given in Tables 3 and 4 were also verified by letting the crack depth to be $10^{-5}b$, where a/b is of order unity.

Table 3. Stress intensity factors for the inside edge crack in a thick-walled cylinder ($a=c<d<b$, Figure 1). $k'(d)=k(d)/\sigma_0\sqrt{d-a}$ (external load: uniform tension $\sigma_{zz}=\sigma_0$), $k'_t(d)=k(d)/\sigma_t\sqrt{d-a}$ (external load: steady-state thermal stress, $\sigma_t=\alpha E(T_0-T_i)/2(1-\nu)$).

d/b	a/b=0.3		a/b=0.8
	k'(d)	k'_t(d)	k'_t(d)
0.30	→1.1215	→1.5333	
0.40	0.9655	1.0120	
0.50	0.9162	0.7099	
0.60	0.9204	0.5027	
0.70	0.9764	0.3498	
0.80	1.1172	0.2323	→1.2046
0.84			0.9671
0.90	1.4981	0.1372	0.7190
0.95			0.4751
1.00	→∞	→0.0	→0.0

Table 4. Stress intensity factors for the outside edge crack in a thick-walled cylinder, $a/b=0.8$ ($a<c<d=b$, Figure 1). $k'(c)=k(c)/\sigma_0\sqrt{b-c}$ (for uniform axial stress $\sigma_{zz}=\sigma_0$), $k'_t(c)=k(c)/\sigma_t\sqrt{b-c}$ (for thermal stress, $\sigma_t=\alpha E(T_i-T_0)/2(1-\nu)$).

c/b	1.00	0.98	0.96	0.94	0.92	0.90	0.85	0.80
k'(c)	→1.1215	1.1615	1.2513	1.3706	1.5141	1.6817		→∞
k'_t(c)	→1.0383	0.9487	0.8905	0.8385	0.7832	0.7189	0.4892	→0.0

plane with an edge crack of depth ℓ under uniform tension σ_0 the stress intensity factor is $1.1215\sigma_0\sqrt{\ell}$ (see, for example, [5]). Thus the expected results are recovered in limit. Table 3 and Figure 2 show that for a fixed a/b as d/b increases starting with a/b , the initial reduction in $k'(d)$ is much more noticeable than the internal crack case. Figure 2 also shows the stress intensity ratio for the penny-shaped crack in an infinite solid, namely $2/\pi$. The dashed line shown in the figure approximates the stress intensity factor ratio $k'(d)=k(d)/\sigma_0\sqrt{d-a}$ in an infinite

solid containing a cylindrical hole and an internal edge crack. It would be expected that for $d-a \ll a$, $k'(d) \rightarrow 1.1215$; for $d \gg a$, $k'(d) \rightarrow 2/\pi$; and, in between, $k'(d)$ would be a monotonically decreasing function of d . This appears to be the reason for the decrease in $k'(d)$ when $d-a$ is small compared to b .

The result for the outer edge crack in a uniformly loaded cylinder is shown in Table 4. Here the stress intensity ratio $k'(c)$ increases quite rapidly with increasing crack depth $b-c$.

For $a/b=0.8$ the edge crack results for the steady-state thermal stress case are shown in Tables 3 and 4. The same results and the thermal stress σ_{zz}/σ_t given by (38) are also shown in Figure 3. It is assumed that $T_o > T_i$ for the inner edge crack and $T_o < T_i$ for the outer edge crack, T_o and T_i being the outer and inner wall temperatures (Figure 3 shows only $T_o > T_i$). Note that (a) the stress intensity factor is always positive if the edge crack starts from the wall which is under tension, (b) it monotonically decreases as the crack depth increases, and (c) it approaches zero as the thickness of the net ligament goes to zero. Basically, this is the same result found in [12] for a strip under (self-equilibrating) residual stresses.

REFERENCES

1. Erdogan, F. and Ratwani, M., "Fracture of cylindrical and spherical shells containing a crack", *Nuclear Engineering and Design*, vol. 20, pp. 265-286, 1972.
2. Collins, W. D., "Some axially symmetric stress distribution in elastic solids containing penny-shaped cracks", *Proc., Edinburgh Math. Soc.* (2), vol. 13, pp. 69-78, 1962.
3. Sneddon, I. N. and Tait, R. J., "The effect of a penny-shaped crack on the distribution of stress in a long circular cylinder", *Int. J. Engng. Sci.*, vol. 1, pp. 391-409, 1963.
4. Sneddon, I. N. and Welch, J. T., "A note on the distribution of stress in a cylinder containing a penny-shaped crack", *Int. J. Engng. Sci.*, vol. 1, pp. 411-419, 1963.
5. Gupta, G. D. and Erdogan, F., "The problem of edge cracks in an infinite strip", *J. Appl. Mech.*, vol. 41, Trans. ASME, pp. 1001-1006, 1974.
6. Love, A. E. H., A Treatise on the Mathematical Theory of Elasticity, Dover Publ., New York, 1944.
7. Erdelyi, A., Tables of Integral Transforms, vol. 2, McGraw-Hill, New York, 1953.
8. Muskhelishvili, Singular Integral Equations, Noordhoff, Groningen, Holland, 1953.
9. Erdogan, F. and Gupta, G. D., "On the numerical solution of singular integral equations", *Quarterly of Applied Mathematics*, vol. 30, pp. 533-547, 1972.
10. Krenk, S., "A note on the use of interpolation polynomial for solutions of singular integral equations", *Quarterly of Applied Mathematics*, vol. 32, pp. 479-485, 1975.
11. Timoshenko, S. and Goodier, J. N., Theory of Elasticity, McGraw-Hill, New York, 1951.
12. Bakioglu, M. and Erdogan, F., "The crack-contact and the free end problem for a strip under residual stress", (to appear in *J. Appl. Mech.*, Trans. ASME, 1977).

APPENDIX

The functions $A_i(s)$, $B_i(s)$, $C_i(s)$, $D_i(s)$, $h_i(t,s)$, ($i=1,\dots,4$), and $\Delta(s)$.

$$A_1 = (-M_1L_2 + M_2L_4)Z_1 ,$$

$$A_2 = (M_1L_1 - M_2L_3)Z_1 ,$$

$$A_3 = M_1[-sL_1Z_5 + L_2(sZ_2 + Z_1/a)] \\ + M_2[-L_4(sZ_2 + Z_1/a) + sZ_5L_3] - \Delta K_1(bs)/Z_1 ,$$

$$A_4 = M_1[L_1(sZ_3 - Z_1/b) - sZ_4L_2] \\ + M_2[sL_4Z_4 - L_3(sZ_3 - Z_1/b)] + \Delta K_1(as)/Z_1 ;$$

$$B_1 = -L_2Z_1 ,$$

$$B_2 = L_1Z_1 ,$$

$$B_3 = -sL_1Z_5 + L_2(sZ_2 + Z_1/a) ,$$

$$B_4 = L_1(sZ_3 - Z_1/b) - sL_2Z_4 ;$$

$$C_1 = (-L_2M_3 + L_4M_4)Z_1 ,$$

$$C_2 = (L_1M_3 - L_3M_4)Z_1 ,$$

$$C_3 = M_3[-sL_1Z_5 + L_2(sZ_2 + Z_1/a)] \\ + M_4[-L_4(sZ_2 + Z_1/a) + sL_3Z_5] - \Delta I_1(bs)/Z_1 ,$$

$$C_4 = M_3[L_1(sZ_3 - Z_1/b) - sL_2Z_4] \\ + M_4[sL_4Z_4 - L_3(sZ_3 - Z_1/b)] + \Delta I_1(as)/Z_1 ;$$

$$D_1 = L_4Z_1 ,$$

$$D_2 = -L_3Z_1 ,$$

$$D_3 = -L_4(sZ_2 + Z_1/a) + sL_3Z_5 ,$$

$$D_4 = sL_4Z_4 - L_3(sZ_3 - Z_1/b) ;$$

$$Z_1 = K_1(as)I_1(bs) - K_1(bs)I_1(as) ,$$

$$Z_2 = I_0(as)K_1(bs) + K_0(as)I_1(bs) ,$$

$$Z_3 = I_0(bs)K_1(as) + K_0(bs)I_1(as) ,$$

$$Z_4 = I_0(as)K_1(as) + K_0(as)I_1(as) ,$$

$$Z_5 = I_0(bs)K_1(bs) + K_0(bs)I_1(bs) ;$$

$$M_1 = [asI_0(as)K_1(bs) - sbI_0(bs)K_1(as) - 2(1-v)Z_1]Z_1^{-1} ,$$

$$M_2 = [-asK_0(as)K_1(bs) + bsK_0(bs)K_1(as)]Z_1^{-1} ,$$

$$M_3 = [asI_0(as)I_1(bs) - bsI_0(bs)I_1(as)]Z_1^{-1} ,$$

$$M_4 = [2(1-v)Z_1 - asK_0(as)I_1(bs) + bsK_0(bs)I_1(as)]Z_1^{-1} ;$$

$$L_1 = as^2[Z_2K_0(as) - Z_1K_1(as)] - bs^2Z_4K_0(bs) - \frac{2(1-v)}{a} Z_1K_1(as) ,$$

$$L_2 = as^2Z_5K_0(as) - bs^2[Z_3K_0(bs) + Z_1K_1(bs)] - \frac{2(1-v)}{b} Z_1K_1(bs) ,$$

$$L_3 = as^2[-Z_2I_0(as) - Z_1I_1(as)] + bs^2Z_4I_0(bs) - \frac{2(1-\nu)}{a} Z_1I_1(as) ,$$

$$L_4 = -as^2Z_5I_0(as) + bs^2[Z_3I_0(bs) - Z_1I_1(bs)] - \frac{2(1-\nu)}{b} Z_1I_1(bs) ;$$

$$\Delta = L_1L_4 - L_2L_3 ;$$

$$h_1 = -s[I_1(as)K_1(ts) \left(\frac{2(\nu-1)}{a} - as^2\right) + s^2tI_0(as)K_0(ts) \\ + sI_0(as)K_1(ts) - \frac{ts}{a} I_1(as)K_0(ts)] ,$$

$$h_2 = -s[I_1(ts)K_1(bs) \left(\frac{2(\nu-1)}{b} - s^2b\right) + ts^2I_0(ts)K_0(bs) \\ - sI_1(ts)K_0(bs) + \frac{ts}{b} I_0(ts)K_1(bs)] ,$$

$$h_3 = -s^2[aI_0(as)K_1(ts) - tI_1(as)K_0(ts)] ,$$

$$h_4 = -s^2[-bI_1(ts)K_0(bs) + tI_0(ts)K_1(bs)] .$$

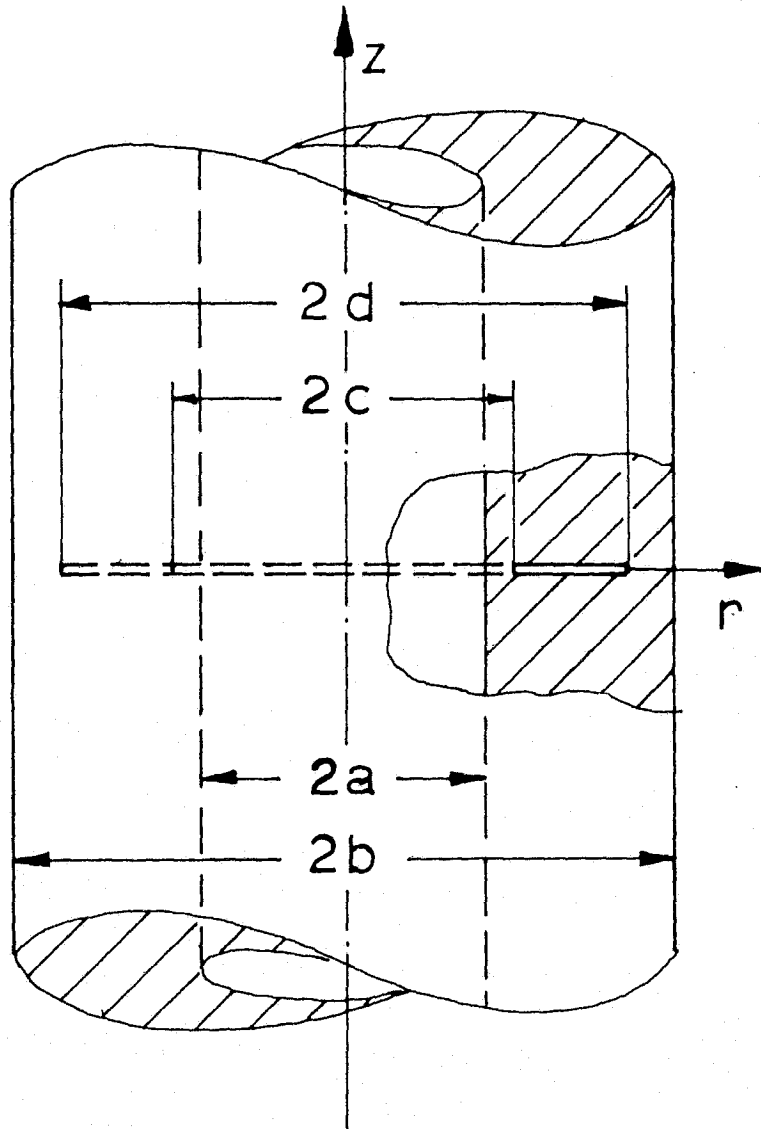


Figure 1. Geometry of a thick-walled cylinder containing a ring-shaped crack.

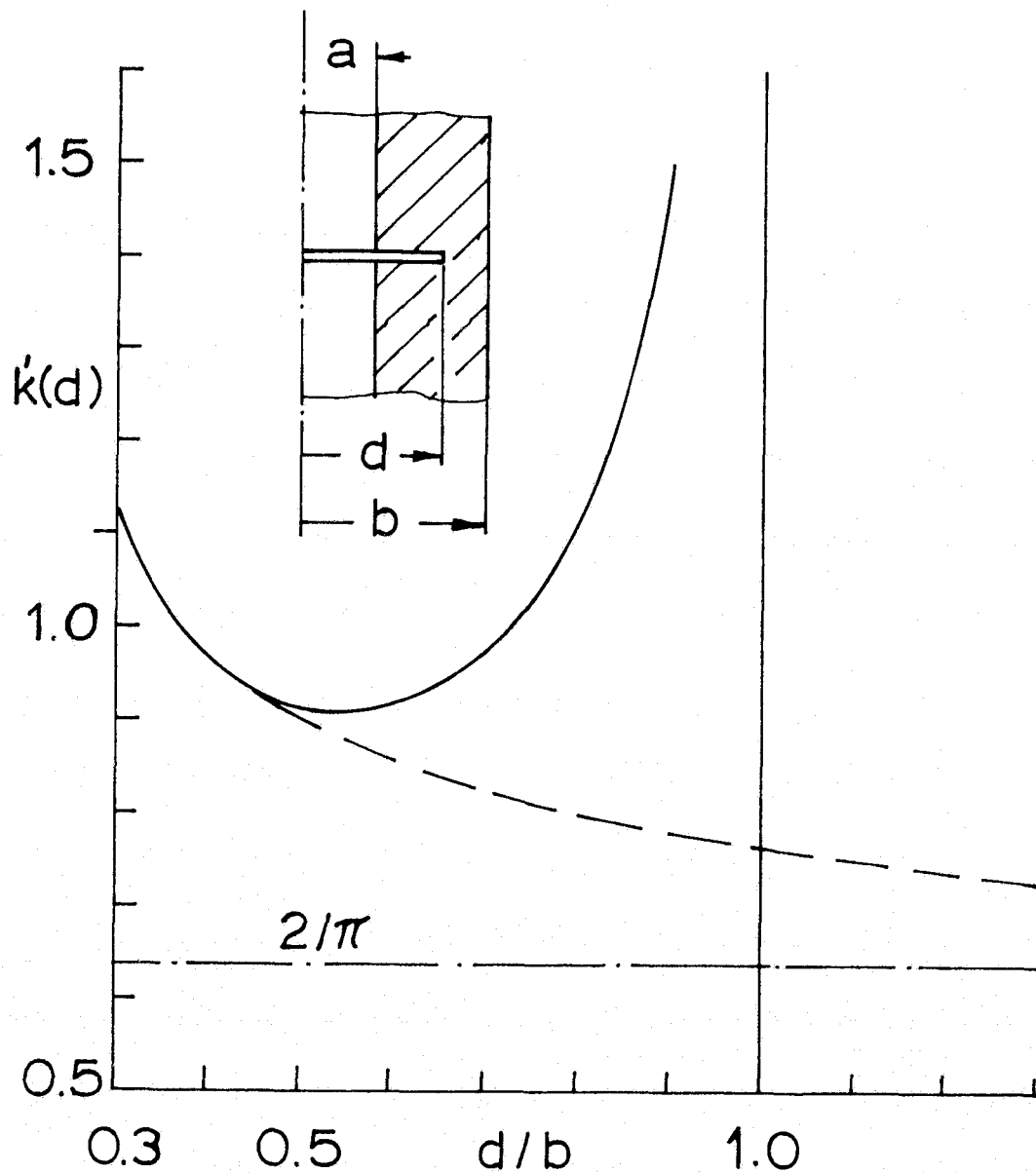


Figure 2. The stress intensity factor for an (internal) edge crack in a thick-walled cylinder under uniform axial stress $\sigma_{zz} = \sigma_0$. $a/b = 0.3$, $k'(d) = k(d)/\sigma_0\sqrt{d-a}$ (the dashed line is the approximate $k'(d)$ for an infinite medium with a cylindrical hole of radius a and an internal edge crack of depth $d-a$).

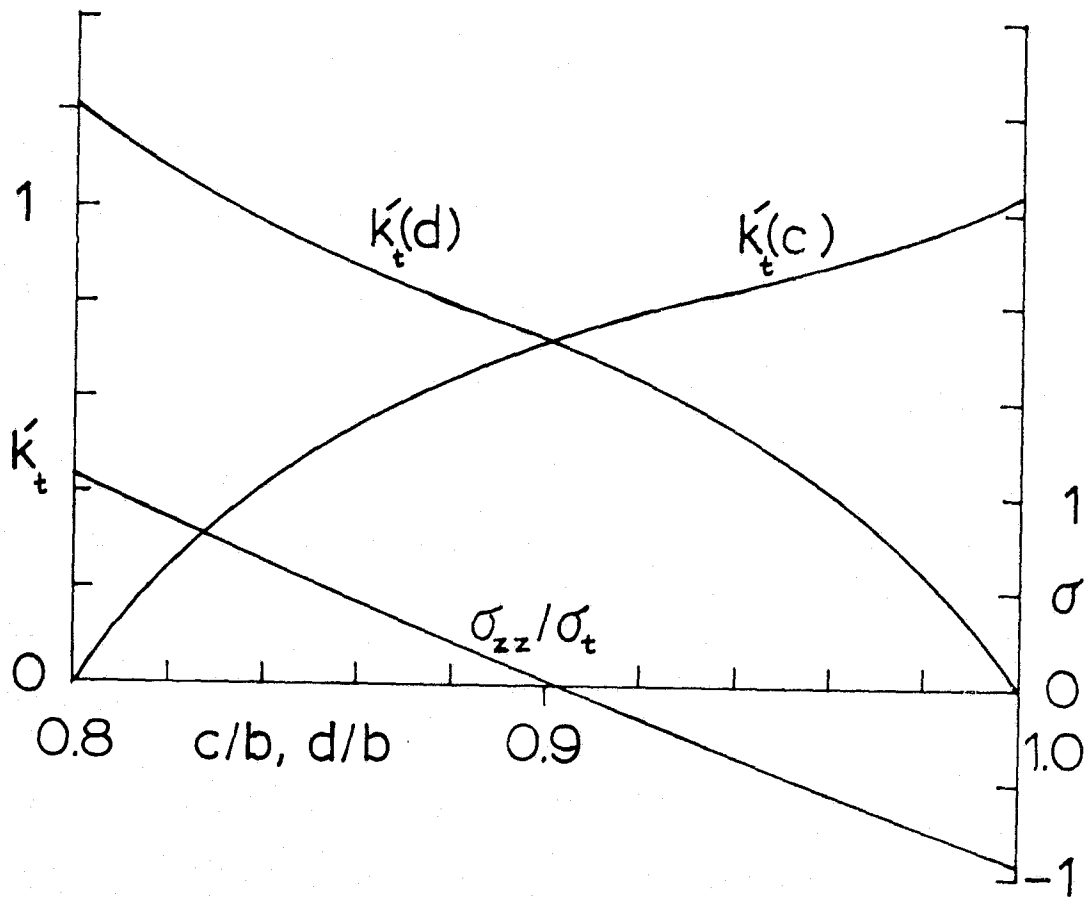


Figure 3. Stress intensity factors for an internal edge crack, $k'_t(d)$, and for an external edge crack, $k'_t(c)$, in a thick-walled cylinder under steady-state thermal stress. $a/b=0.8$, $k'_t(d)=k(d)/\sigma_t\sqrt{d-a}$, $k'(c)=k(c)/\sigma_t\sqrt{b-c}$, $\sigma_t=\alpha E|T_0-T_i|/2(1-\nu)$.